Multi-Disciplinary Senior Design Conference
Kate Gleason College of Engineering
Rochester Institute of Technology
Rochester, New York 14623

Project Number: P09051

COST-EFFECTIVE OXYGEN GAS SENSOR VIA FLUORESCENCE QUENCHING

Samuel Shin/ EE **Jeremy Goodman/ uE**

ABSTRACT

The goal of this project is to design and build a cost-effective oxygen sensor through the use of fluorescence spectroscopic analysis on the Tris(2,2'bipyridal)dichlororuthenium(II) compound and low-cost support electronics. The objective of the project is to generate a Stern-Volmer chart and demonstrate the oxygen-quenching effect on fluorescent intensity and lifetime. A customized P-I-N photodiode, designed and fabricated in the RIT Semiconductor and Microsystems Fabrication Laboratory (SMFL), is used to measure the emitted fluorescent signal.

Keywords: Oxygen Sensor, Fluorescence, Fluorometry, Spectrofluorometry, PIN Photodiode, Tris Ruthenium(II)

NOMENCLATURE

$Ru(bpy)_3^{2+}$: Tris(2,2'bipyridal)dichlororuthenium(II)
Fluorophore: Fluorescence-emitting material
PMT: Photomultiplier Tube
Fluorometry: Fluorescence Spectroscopy
SMFL: Semiconductor and Microsystems Fabrication Laboratory
LED: Light-Emitting Diode

INTRODUCTION

The measurement of molecular oxygen concentration in a gaseous or liquid environment is vital to biomedical and environmental analysis. Oxygen sensing via fluorescence spectroscopy requires the use of oxygen quenching fluorophores (fluorescent materials sensitive to oxygen concentration), as well as excitation and recording devices to induce and measure the emitted fluorescence. Photomultiplier tubes (PMT) are commonly used as recording devices in fluorometry; however, PMTs are historically expensive and require large external power supplies to operate, making the sensor unavailable to the average consumer. The use of low-cost silicon photodetectors have decreased the product cost greatly but lack the precision PMTs give to the technique.

Ruthenium-based materials have historically been used for oxygen sensing due to their dynamic fluorescence quenching with the incorporation of molecular oxygen. For this project, the Tris(2,2'bipyridal)dichlororuthenium(II) compound was used as the oxygen sensing material incorporated in a silicone polymer matrix. These materials take advantage of the oxygen diffusion properties of the silicone polymer to readily incorporate oxygen into the film when in the presence of oxygen, and out-diffuse when in the absence of oxygen. The oxygen sensing material was acquired from Sigma-Aldrich and the silicone polymer (Permatex Clear Silicon RTV66B) was acquired from Grainger Industrial Supply.

The goal of this project is to develop a prototype oxygen sensor based on the dynamic fluorescent quenching behavior of the Tris(2,2'bipyridal)dichlororuthenium(II) molecule and examining the oxygen sensing capabilities through the use of low-cost fluorescence spectroscopy techniques. The oxygen measuring capabilities of the prototype sensor will be judged through noticeable changes in the sensor when subject to open-air and 0% oxygen. The objective of the project is fulfilled following visible fluctuations in sensor output over different quantities of oxygen concentration. A Stern-Volmer Characteristic Plot will be generated from the recorded data that will be used to judge the oxygen quenching capabilities of the Tris(2,2'bipyridal)dichlororuthenium(II) molecule, as well as the operation of the sensor itself.

THEORY

1. Dynamic Oxygen Quenching and Ru(bpy)$_3^{2+}$

Molecular oxygen measurement has been used for many years and has many different techniques available to use. The use of fluorescent materials sensitive to oxygen concentration is a lucrative venture; one family of materials available, the Ruthenium-based ligands displays a strong fluorescent reaction to differing levels of oxygen concentration.

Oxygen quenching is a phenomena which affects materials like Tris(2,2'bipyridal)dichlororuthenium(II) [Ru(bpy)$_3^{2+}$], shown in Fig. 1, which emit fluorescence through a physical phosphorescent reaction. For Ru(bpy)$_3^{2+}$, incident radiation at 455nm (royal blue) will excite the material enough to emit fluorescence at a wavelength of 613nm (orange-red).

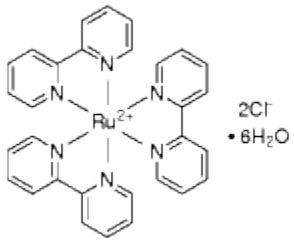

Figure 1. Tris(2,2'bipyridal)dichlororuthenium(II) molecule

Oxygen atoms are greatly attracted to the Ruthenium-complex, making molecular collisions more likely in higher oxygen-concentration environments. When the oxygen atom strikes the fluorescing Ruthenium-complex, a change in energy occurs causing the Ruthenium-complex to stop fluorescence. Fig. 2 shows the process of dynamic (collisional) oxygen quenching of Ruthenium-based complexes. In the absence of molecular oxygen, the fluorescent intensity will be at its maximum, and intensity will decrease with increasing oxygen concentration.

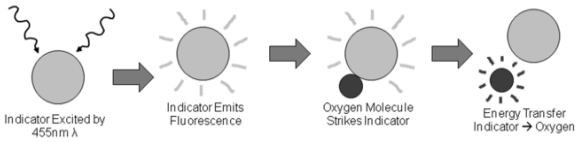

Figure 2. Dynamic Fluorescence Quenching by Oxygen Atom Through Collision Quenching

Historically, the measure of the dynamic fluorescence quenching capabilities of a material is shown through the Stern-Volmer relationship, for both fluorescent lifetime and intensity, shown in Eq. (1) and (2), respectively [1].

$$\tau_0/\tau = 1 + K_{sv}[O_2] \quad (1)$$

$$I_0/I = 1 + K_{sv}[O_2] \quad (2)$$

$\tau_0/\tau : Relative\ Fluorescent\ Lifetime$
$I_0/I : Relative\ Fluorescent\ Intensity$
$K_{sv} : Stern - Volmer\ Constant$
$[O_2] : Concentration\ of\ Oxygen\ in\ System$

2. Photodiode Construction and Operation

A. Photodiode as PN-Junction

A photodiode is a semiconductor device used to convert photonic energy into an electric current, or photocurrent. Photodiodes are commonly explained using a p-n junction approach. When two types of semiconductor materials, n-type and p-type, are joined together, an area known as a depletion region is created at the interface. When a photon strikes the P-N-junction, energy is transferred into the crystal structure. If the energy of the photon is larger than the band-gap energy of the material, an electron will be "ejected" from the valence band of the material. Once an electron is ejected, a hole remains. This electron-hole pair generation is the driving force behind the operation of a photodiode.

In principle, electrons will be attracted to positive polarity, while the positive charges, or holes, will be attracted to negative polarity. From the point of electron-hole pair generation, the electrons will flow towards the P-region of the device while the holes will flow to the N-region. As more photons strike the surface and create more electron-hole pairs, more electrons will flow to the positive regions and the holes will flow to the negative, thus creating a flow, or photocurrent, in the device. This phenomenon is shown in Fig. 3.

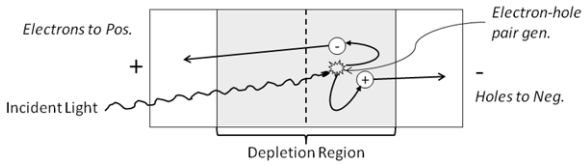

Figure 3. PN Junction showing photon absorption and electron/hole pair generation

The depletion region generated at the interface provides an area of high electric-field in the p-n junction. If the electron-hole pair is generated in the depletion region, the large electric-field present will accelerate the flow of particles to a rate far greater than if they were generated in the P- or N-regions. The highest particle flow will occur in the depletion region; therefore, it is beneficial for the photodiode designer to match the depletion region depth to the absorption depth associated with the wavelengths being collected. When the photodiode is reverse-

biased, the depletion region thickness and ε-field will increase in magnitude, increasing the flow-rate of charges absorbed in the region; therefore, increasing the photonic response time of the device.

As a larger reverse-bias voltage is placed on the photodiode, the photocurrent will be slightly increased while the response time will be significantly increased. Additionally, as more light is applied to the photodiode, the current produced will be increased. An example of an I-V characteristic of a photodiode is shown in Figure 4.

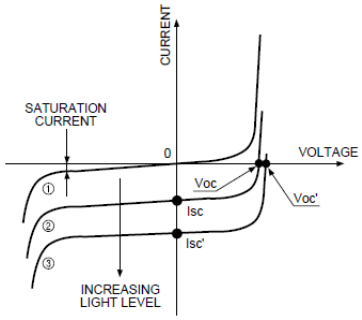

Figure 4. Output of photodiode given increasing incident light [2]

B. Photodiode Responsitivity

For a photodiode, the conversion of photonic energy to photocurrent is not a loss-less process. Because photonic energy can be absorbed in the N- and P-regions, as well as the depletion region, the ratio of generated electron-hole pairs to absorbed photons is never exactly unity. The ratio of electron-hole pairs generated to photons absorbed is known as the internal quantum efficiency, η. The internal quantum efficiency of the photodiode is largely dependent on the absorption coefficient of the semiconductor material and thickness of the absorbing region [3]. Therefore, the photocurrent response of the photodiode, shown in Eq. (3), is largely reliant on the quantum efficiency and absorption magnitude at a given wavelength.

$$R = \frac{I_{ph}}{P_{inc}} = \frac{\eta q}{h\nu} \tag{3}$$

$I_{ph}: Photocurrent$
$P_{inc}: Incident\ Photonic\ Power\ on\ Photodiode$
$\eta: Quantum\ Efficiency$
$q: Charge\ of\ an\ Electron$
$h\nu: Energy\ of\ Light\ according\ to\ wavelength$

C. *Photodiode Response Time*

The rate and density of data transmission depend on the response speed of the photodiode [3]. The photocurrent is defined as the flow of electrons and holes to their respective contacts, the parameter defined as the time elapsed between electron-hole generation and the collection of a charge at the electrode is known as photonic response time. Like all time-based circuits, the photodiode response time is based off of its RC- time constant. A large capacitance or resistance in the device will cause the response time of the circuit to increase, a phenomenon that is detrimental to the performance of the photodiode.

The depletion layer of a p-n junction can be viewed as a parallel plate capacitor with its capacitance given as the ratio of the depletion layer area to the depletion layer width [3].

$$C = \frac{\epsilon_s \epsilon_0 A}{W} \tag{4}$$

$C: Depletion\ Layer\ Capacitance$
$\epsilon_s\ and\ \epsilon_0: Permittivity\ of\ silicon\ and\ freespace$
$A: Photodiode\ Active\ Area\ Size\ (Photoabsorbing)$
$W: Depletion\ Layer\ Width$

The capacitance generated in this layer is known as the junction capacitance. Observing the AC representation of the photodiode, shown in Figure 5, the junction capacitance, cj, and shunt and series resistance, Rsh and Rs, is in parallel to the generated photocurrent, Io. These components make up the capacitance and resistance that define the RC-time constant.

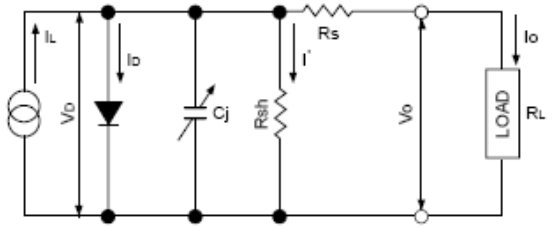

Figure 5. AC representation of P-I-N photodiode [2]

It is possible to minimize the junction capacitance of the photodiode by decreasing the overall area and increasing the thickness of the depletion layer. By increasing the thickness of the depletion layer, the ε-field will occupy a larger space in the semiconductor and effectively lowers the resistance inside it. With a decreased resistance and a decreased capacitance (through a smaller active area size), the RC-time constant of the photodiode will be minimized. In practice, planar photodiodes are able to achieve very high photonic response times by tuning the size of the active area to very small dimensions, often to less than $1mm^2$.

EXPERIMENTAL PROCESS

1. $Ru(bpy)_3^{2+}$ Film Preparation

Tris(2,2'bipyridal)dichlororuthenium(II) hexahydrate powder was purchased from Sigma-Aldrich for use as the oxygen label in the sensing film. A stock solution of the material was made from dissolving 5mg of dry $Ru(bpy)_3^{2+}$ in 40mL of methanol [0.2mM solution]. In a separate container, 0.5g of silicone was dissolved in 3mL of toluene to increase the support matrix viscosity and aid in the absorbance of the stock solution. A 1mL sample of stock solution was transferred to the silicone solution and agitated for 1 minute using a megasonic agitator. A 0.3mL sample was then extracted from the mixture and placed on an optical-grade microscope slide. The film was left to dry in open air for 24-hours before handling.

2. Photodiode Fabrication (RIT SMFL)

In conjunction with the Microelectronic Engineering Department and the Semiconductor and Microsystems Fabrication Laboratory (SMFL), two photodiode architectures, lateral and planar, were designed and built for incorporation in the O_2-sensor system. Based on their individual performance, the most-desirable photodiode architecture is integrated into the O_2-sensor prototype.

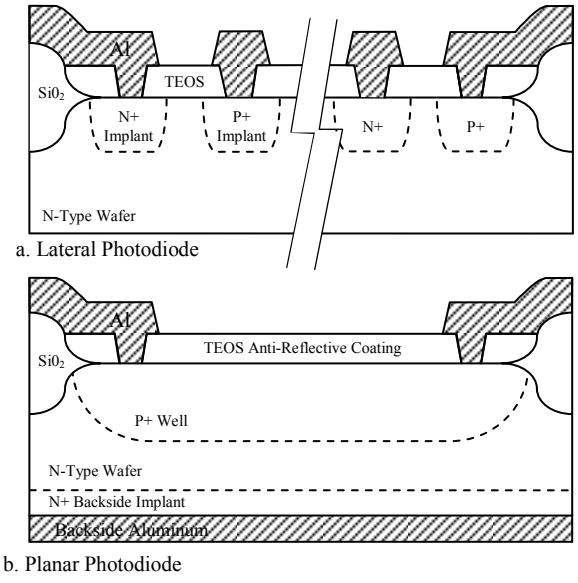

Figure 6. Cross-section Diagrams of Photodiode Architectures Fabricated in RIT SMFL. Lateral Photodiode, a, and Planar Photodiode, b, respectively.

Fig. 6 displays the cross-sectional representation of the two photodiode architectures being constructed. Both architectures used a 5-level lithography process and included a 100nm TEOS film serving as an anti-reflective coating for the device. The design layout of the devices is shown in Fig. 7.

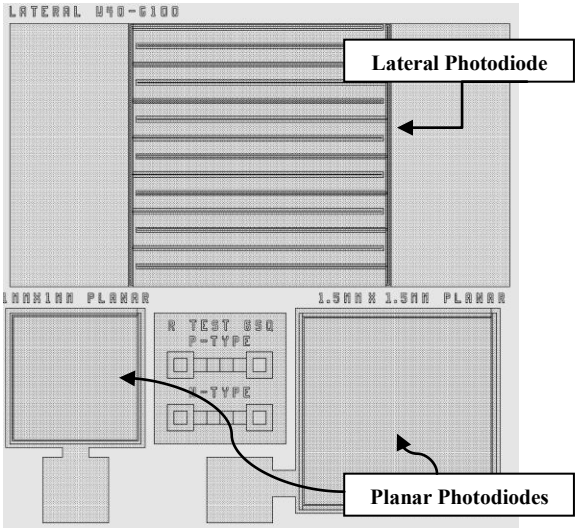

Figure 7. Design Layout of Lateral/Planar Photodiode Die

Each device is tested for their respective I-V and C-V characteristics, photonic response, and rise/fall time. The lateral and planar photodiodes, based on their construction either excel or fall-short in these areas.

3. Assembly of the Emitter/Receiver

The LED emitter system is created with the purpose of operating a gate-controlled LED to excite a fluorescence reaction in the oxygen sensitive thin-film. The functional diagram explaining the operation is shown in Figure 8.

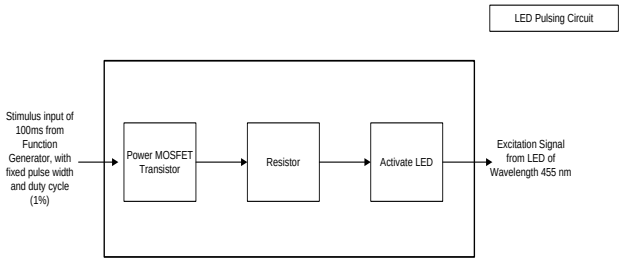

Figure 8. Functional decomposition diagram for the LED emitter circuit.

A. Input Voltage Source

A signal generator is used to drive the gate-control function of the LED emitter assembly. The emitter is assembled using a PMOSFET; therefore, the gate is opened by passing a negative threshold voltage. The signal generator can be used to set a pulse-signal to the gate, opening and closing over a set duty cycle. In order to measure time-resolved fluorescence, the pulse width is specifically set to a ratio of 1% of the total period – this provides the system a fast pulse and a long rest-phase, allowing the fluorescence signal to cease before exciting the material again.

B. *Power MOSFET Transistor*

In order to produce a voltage-driven switch, a PMOS-gated circuit was used. Using the IRF4905 PMOSFET device, the gating control was able to achieve nano-second switching times while handling up to 3 Watts of power.

C. *Resistor*

A current limiting resistor is used to ensure small increments of current are being applied to the LED. A 100Ω resistor is used in the LED emitter assembly.

D. Light Emitting Diode

A Luxeon III LED is used as the excitation source for the oxygen sensor system. The 455nm LED has a rise time of less than 100nano-seconds while maintaining a long operating life. The reliability and performance made this LED a prime candidate for the oxygen sensor system.

4. Operation of the Receiver

The photodiode is used to receive the generated fluorescence emitted from the oxygen sensitive thin-film following excitation by the LED. The output current is converted to a voltage for measurement on an oscilloscope. A functional decomposition diagram for the receiver circuit is shown in Figure 9.

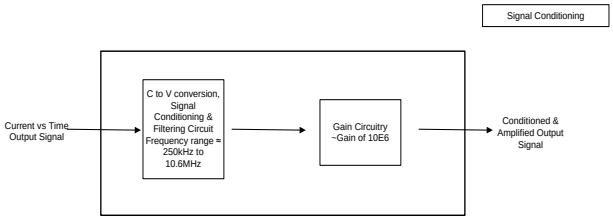

Figure 9. Functional Decomposition Diagram for the Receiver Circuit.

A. *Transimpedance amplifier & signal conditioning*

The current generated through absorption of fluorescent photons following fluorescence excitation is fed through a transimpedance amplifier, converting the current to a voltage. The conversion can amplify the signal based on the value of the feedback resistor. Signal conditioning can be added to the system to remove unwanted noise caused by the power source or other outside factors.

B. *Gain Circuitry*

The projected voltage range of the photodiode output is in the order of microamps. In order to have a viewable output, a gain of 1,000,000 is used in the transimpedance amplifier in order to observe changes in device output. An inverse-gain circuit configuration was used, as seen in Eq. (5)

$$\frac{-R_F}{R_1} = \frac{V_{out}}{V_{in}} = Gain \tag{5}$$

5. Assembly of Emitter & Receiver

The circuits are simulated using Orcad Pspice. Following successful simulation, each device is constructed on individual Vectoboards for final assembly. Circuit diagrams of the LED emitter assembly and photodiode transimpedance amplifier is shown in Figures 10 and 11, respectively.

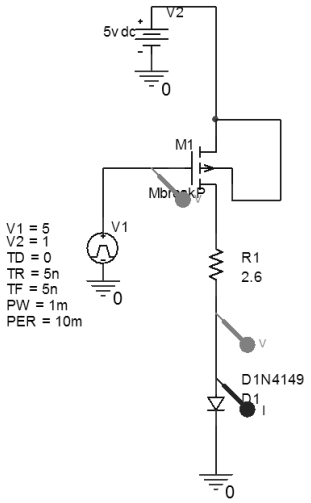

Figure 10. Circuit Digram of LED Emitter Circuit.

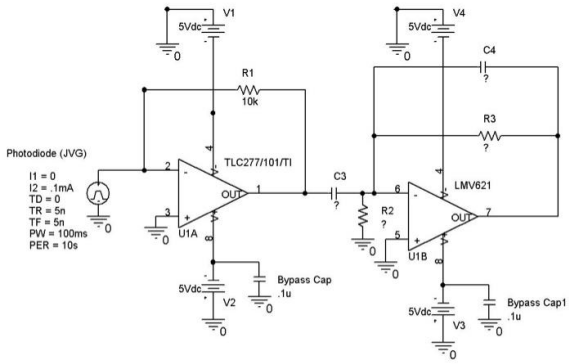

Figure 11. Circuit Diagram of the Transimpedance Amplifier.

TEST PLAN

1. Verification of the Emitter & Receiver Operation

The emitter and receiver circuits are tested to observe proper operation; for example, closely checking for desired rise- and fall-time to verify ability to perform time-resolved analysis. Most of the operations were executed using varying pulse widths and input signal magnitudes, in order to verify operation of the emitter. The receiver circuit is tested by mounting a commercially-available photodiode to the receiver circuit. Using varying LED pulses, the emitted light is received by the photodiode and a voltage response difference is observed. Rise- and

fall-time response of the photodiode is tested in this manner, also.

2. Verification of Fabricated Photodiode Operation

Each fabricated device is subject to on-wafer testing before device packaging. After package, an I-V characteristic is generated using the HP4145 Parameter Analyzer under increasing light levels. C-V characteristics are then gathered using the capacitance probe station in the Microelectronic Engineering Department Device Test Lab. Spectral analysis is performed on the device to determine the responsitivity of the photodiode to changes in incident wavelength. Lastly, device rise/fall times are measured using the SOP3202A Oscilloscope and a 10kHz signal pulsed through a 455nm Philips LumiLEDs high-power LED.

3. Assembly of System

The system is constructed following the design shown in Figure 12.

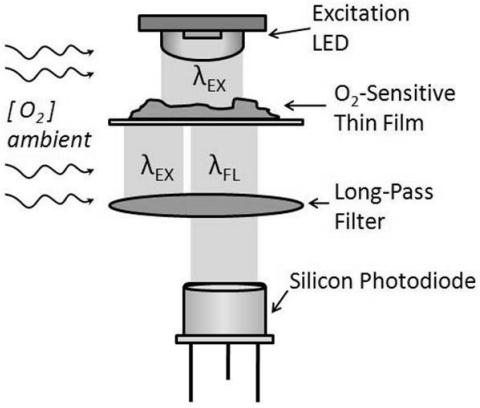

Figure 12. Construction Assembly for Oxygen Sensor

The LED pulsing assembly is mounted above the oxygen-sensing material. The optical filter is placed above the photodiode and is intended to pass the fluorescence wavelength while filtering out the extraneous LED light.

4. Test Phase I

The oxygen sensor assembly is placed in a sealed (light-tight) container with hardware/display devices external to the unit. The LED is activated in steady-state mode to excite the oxygen-sensing film, which is currently affected by open-air oxygen concentrations. The resulting fluorescence is recorded by the photodiode. An initial, "set-point", measurement is taken with open-air oxygen levels. The container is then purged for 1 minute with nitrogen gas. The resulting signal for 0% oxygen is recorded.

A change in output signal magnitude as a result of varying oxygen levels will verify oxygen quenching of the sensing film and proper operation of the support electronics.

5. Test Phase II

A. Test Chamber

A test chamber is constructed which allows adjustment of nitrogen and oxygen gas flow to measure sensor response at varying oxygen concentrations. Figure 13 shows the test schematic and chamber construction diagram for the flow chamber.

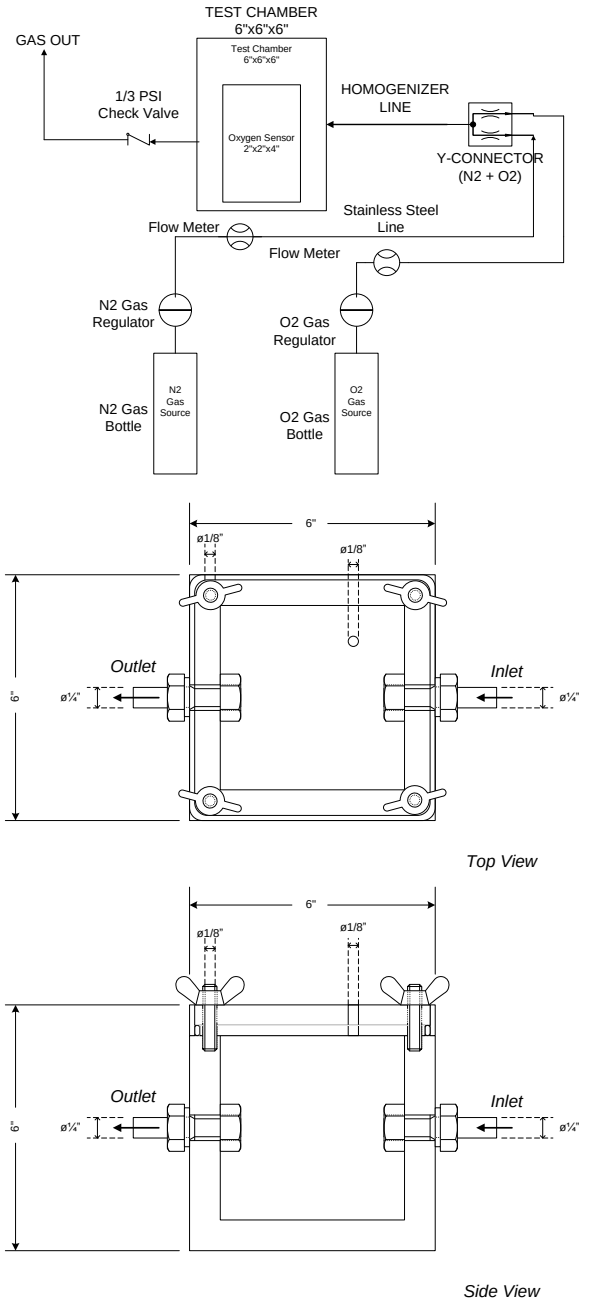

Figure 13. Test System/Flow Chamber Specifications

Using the flow meters, a known ratio of gas can be passed through the system, exiting through the use of a 1/3PSI check valve.

B. Sensor Operation and Measurement

The assembled oxygen sensor is placed inside the test system. Oxygen concentration is altered by changing the flow rates of oxygen and nitrogen gases. A measurement from the photodiode is taken at 10% increments of oxygen concentration.

Using the intensity data gathered through this technique, a Stern-Volmer characteristic plot is generated by inputting the data into Eq. (2).

RESULTS AND DISCUSSION

A. Oxygen Sensing Film Preparation

The Tris(2,2'bipyridal)dichlororuthenium(II) thin film was generated with the help of the RIT Chemistry Department staff. Clear silicone was used as a support matrix for the sensor while allowing high oxygen permeability to promote oxygen diffusion through the film. Two plates of film were prepared.

B. Custom Photodiode

Two photodiode architectures were created in the RIT SMFL. Both were tested successfully for responsivity and junction capacitance. The planar photodiode had roughly two-times the responsivity of the lateral; however, the junction capacitance arising from the large active area made time-resolved measurements impossible. The lateral photodiode had limited responsivity but had decreased capacitance allowing for greater versatility in time-resolved sensing methods. Although the planar photodiode is the likely candidate for incorporation into the oxygen sensor, neither device was incorporated into the final prototype.

C. Support Electronics

The support electronics were constructed successfully using Vectoboard circuit boards to mount the individual components, shown in Figure 14.

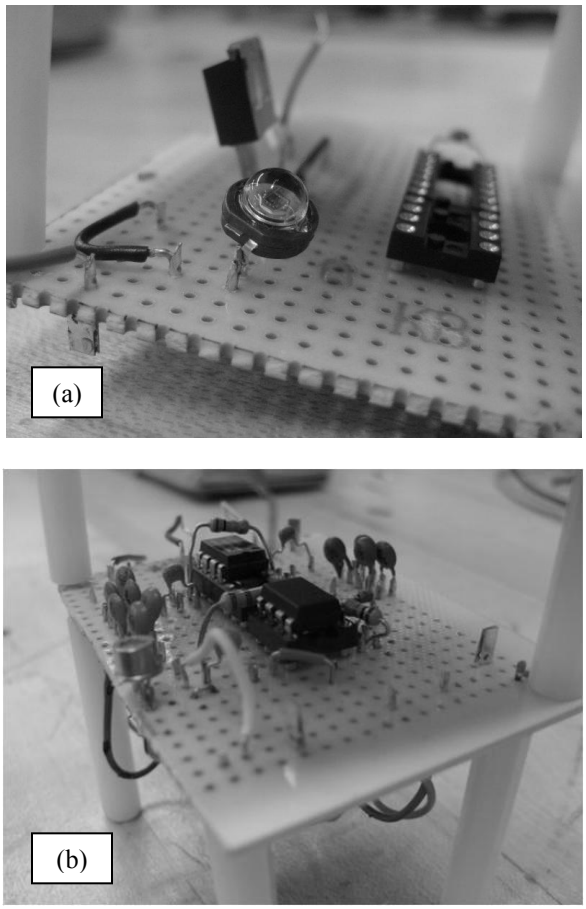

Figure 14. Vectoboard Construction of LED, (a), and Photodiode, (b), support electronics

Each board verified proper operation. The LED was assembled to allow steady-state or time-varying operation to account for intensity or lifetime measurement methods. Only intensity measurements were used in the project; however, the option still remains.

D. Completed Assembly and Testing

The complete system is shown in Figure 15.

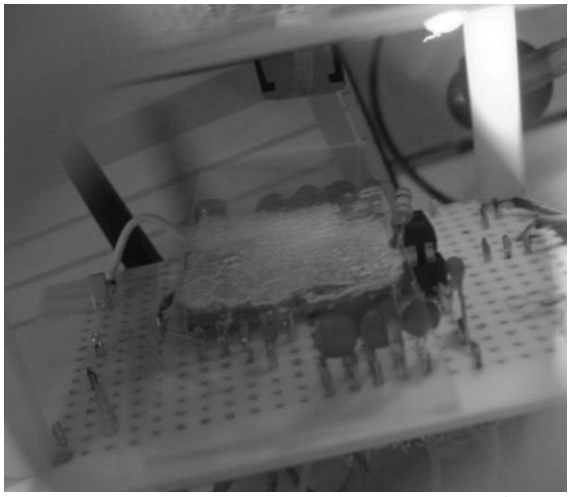

Figure 15. Ru(bpy) Excited by LED, shown through filter

Using a nitrogen source in the RIT SMFL and a light-tight container, test phase I was accomplished by witnessing a 5mV change between room oxygen and 0% Oxygen concentrations. The test chamber was not constructed; therefore, test phase II was not accomplished.

CONCLUSIONS AND RECOMMENDATIONS

The oxygen sensor was successfully constructed using the materials available. The theory was verified through test phase I; however, test phase II was not executed.

Future considerations should be judged on the results of this project. Considerations may include, using a photomultiplier tube for more accurate fluorescence collection, using fiber-optics to reduce outside noise interference, using a higher-quenching agent, such as Tris(4,7-diphenyl-1,10-phenanthroline)ruthenium(II), and delegating the construction of the test chamber as a much higher priority.

This project served to prove the theory of oxygen sensing via fluorescence quenching. Further work is needed to increase sensitivity and versatility of the device, as well as characterize the quenching ability of the oxygen sensitive thin-film used.

REFERENCES

[1] Campbell, A. and D. Uttamchandani, 2004, "Optical Dissolved Oxygen Lifetime Sensor Based On Sol-Gel Immobilisation," IEE Proc.-Sci. Meas. Technol., **151**(4), pp. 291-297.
[2] Hamamatsu Corporation, 2008, Photodiode Technical Information, Hamamatsu Photonics - Europe and America, http://sales.hamamatsu.com/assets/applications/SSD/photodiode_technical_information.pdf.
[3] Bhattacharya, P., 1994, *Semiconductor Optoelectronic Devices*, Prentice Hall, Englewood Cliffs, NJ.

ACKNOWLEDGMENTS

Prof. George Slack, Jayadevan Radhakrishnan, Dr. David Borkholder, Dr. Sean Rommel, Electrical Engineering and Microelectronic Engineering Departments, RIT Semiconductor and Microsystems Fabrication Laboratory staff, Dr. Christopher Collison, RIT Chemistry Department, Rich Deneen, Hamamatsu Photonics